

# Hypergraph reconstruction from network data

Jean-Gabriel Young,<sup>1</sup> Giovanni Petri,<sup>2</sup> and Tiago P. Peixoto<sup>3,2,4</sup>

<sup>1</sup>*Center for the Study of Complex Systems, University of Michigan, Ann Arbor, Michigan 48109, USA*

<sup>2</sup>*ISI Foundation, Via Chisola 5, Torino 10126, Italy*

<sup>3</sup>*Department of Network and Data Science, Central European University, Budapest H-1051, Hungary*

<sup>4</sup>*Department of Mathematical Sciences, University of Bath, Bath BA2 7AY, United Kingdom*

(Dated: November 4, 2021)

Networks can describe the structure of a wide variety of complex systems by specifying how pairs of nodes interact. This choice of representation is flexible, but not necessarily appropriate when joint interactions between groups of nodes are needed to explain empirical phenomena. Networks remain the de facto standard, however, as relational datasets often fail to include higher-order interactions. Here, we introduce a Bayesian approach to reconstruct these missing higher-order interactions, from pairwise network data. Our method is based on the principle of parsimony and only includes higher-order structures when there is sufficient statistical evidence for them.

## I. INTRODUCTION

Empirical networks are often locally dense and globally sparse [1]. Whether they are social, biological, or technological [2], they comprise large groups of densely interconnected nodes, even when only a small fraction of all possible connections exist. This situation leads to delicate modeling challenges: How can we account for two seemingly contradictory properties of networks—density and sparsity—in our models?

Abundant prior work going back to the early days of social network analysis [3, 4] and network science [5, 6] suggests that higher-order interactions [7] are a possible explanation for the local density of networks [1, 6]. According to this reasoning, entities are connected because they have a shared context—a higher-order interaction—within which connections can be created [8]. It is clear that a phenomenon along these lines occurs in many social processes: scientists appear as collaborators in the Web of Science because they co-author papers together; colleagues exchange emails because they are part of the same department or the same division of a company. It is also known that similar phenomena explain tie formation in a broader range of networked systems, including biological, technological or informational systems [7].

The ubiquity of higher-order interactions provides a simple and universal explanation for the observed structure of empirical networks. If we assume that most ties are created within contexts of limited scopes, then the resulting networks are locally dense, matching empirical observations [1, 9, 10].

Despite their tremendous explanatory power, higher-order interactions are seldom used directly to model empirical systems, due to a lack of data [7]. Indeed, while the context is directly observable for some systems—say, co-authored papers or co-locating species—it is unavailable for several others, including brain data [11], typical social interaction data [12], and ecological competitor data [13] to name only a few.

As a specific motivating example, consider one of the empirical social networks gathered as part of the

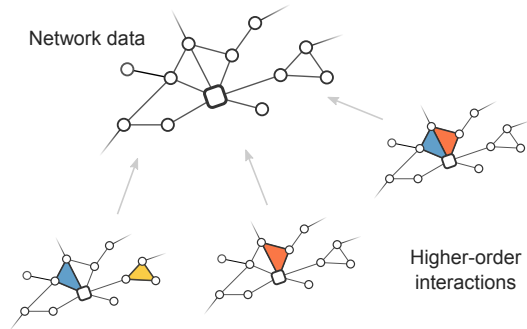


FIG. 1. Extended ego network of a participant of the AddHealth study [14]. Friendships are measured between pairs of participants, even when the fundamental units are groups of friends [12]. Multiple combinations of groups and isolated friendships lead to the same data.

US National Longitudinal Study of Adolescent to Adult Health [14]. This dataset is constructed using surveys, where participants are asked to nominate their friends. Even though there are good reasons to believe that people often interact because of higher-order groups [12], the survey cannot reveal these groups as it only inquires about pairwise relationships. If we actually need the higher-order interactions to give an appropriate description of the social dynamics at play [12], what should we do with such inadequate survey data? As we show in Fig. 1, there are many kinds of higher-order interactions that are compatible with the same network data. How can we pick among all these possible higher-order descriptions?

In the present work, we argue that it is possible to deduce and disambiguate higher-order representations using network data only. In other words, we claim that given a network as input, we can use a parsimonious model to identify the parts of the network best explained by latent higher-order interactions.

We emphasize that this type of inference is distinct from community detection [15, 16], whose goal is to identify the large-scale structure of a network. Community

detection usually delineates large and relatively sparsely connected groups of nodes as coherent subunits of a network. Here, instead, we aim to uncover high-order interactions in networks; in doing so, we decompose the networks in small and fully connected building blocks.

There is prior work on higher-order interaction discovery in network data. As illustrated by Fig. 1, higher-order interactions manifest themselves as cliques—fully connected subgraphs—in network data where they are not recorded explicitly. A common discovery strategy makes use of this fact and equates cliques with higher-order interactions [17–19]. The resulting method is straightforward to implement because it relies on clique enumeration, a classical problem for which we have exact [20, 21] and sampling [22] algorithms that work well in practice. However, clique decompositions do not offer a satisfactory solution to the recovery problem alone. Networks typically admit many possible clique decompositions, which begs the question of which one to pick. For example, a triangle can be decomposed as a single 2-clique, or as three 1-cliques (i.e., as edges); see Fig. 1. In general, the multiplicity of possible solutions implies that higher-order interaction recovery is an *ill-posed inverse problem*. It becomes well-posed only once we add further constraints on what constitutes a good solution.

Existing approaches address the ill-posed nature of the higher-order interaction recovery problem in various ways. For instance, in graph theory, it is customary to look for a minimal set of cliques covering the network [23, 24]. Other methods appeal to notions of randomness and generative modeling to regularize the problem [1, 25]. These methods describe an explicit process by which one goes from higher-order data to networks, and can therefore assign a likelihood to possible higher-order data representations. Our own work is along the same lines but differs from the closest existing approaches, both in its methodological details and philosophical underpinning.

Wegner [25] uses a notion of *probabilistic subgraphs covers* to induce distributions over possible decomposition in motifs. Recent work in graph machine learning also harnesses similar ideas and approaches the problem from a compression perspective [26, 27]. Unlike these authors, we are interested in higher-order interactions only, so the solution space we consider is not the same. We also differ on a methodological ground: we embrace the complexity of the problem and propose a fully Bayesian method that can account for the multiplicity of descriptions, in contrast with the greedy optimization favored in Ref. [25–27]. As a result of these methodological choices, our work is perhaps closest to that of Williamson and Tec [1], who also solve a similar problem from using Bayesian nonparametric techniques [1], and view a network as collections of overlapping cliques. Unlike these authors, however, we think of the network data as uncorrupted; in our framework, latent higher-order interactions always show up in network data as fully connected cliques. In contrast, they think of this process as noisy,

so latent higher-order interactions can translate into relatively sparsely connected sets of nodes. Their methods bear a resemblance to overlapping community detection techniques as a result [16, 28–30].

## II. GENERATIVE MODEL AND INFERENCE

The problem we solve is illustrated in Fig. 1. We have a system we believe is best described with higher-order interactions, but we can only view its structure through the lens of pairwise measurements (an undirected network  $G$ ); our goal is to reconstruct these higher-order interactions from  $G$  only.

For convenience, we encode the higher-order interactions with a *hypergraph*  $H$  [31]. We represent a higher-order interaction between a set of  $k$  nodes  $i_1, \dots, i_k$  with a *hyperedge* of size  $k$ . Empirical data often contain repeated interactions between the same group of nodes, so we use hypergraphs with repeated hyperedges and encode the number of hyperedges connecting nodes  $i_1, \dots, i_k$  as  $A_{i_1, \dots, i_k} \geq 0$ .

Our method then makes use of a Bayesian generative model to deduce one such hypergraph  $H$  from some network dataset  $G$ . This generative model gives an explicit description of how the network data  $G$  is generated when there are latent higher-order interactions  $H$ . With a generative model in place, we can compute the posterior probability

$$P(H|G) = \frac{P(G|H)P(H)}{P(G)} \quad (1)$$

that the latent hypergraph is  $H$ , given the observed network  $G$ . In this equation,  $P(G|H)$  and  $P(H)$  define our generative model for the data, and its evidence  $P(G) = \sum_H P(G|H)P(H)$  functions as a normalization constant.

The appeal of such a Bayesian generative formulation is that we can use  $P(H|G)$  to make queries about the hypergraph  $H$ . What was the most likely set of higher-order interactions? What is the probability that a particular interaction was present in  $H$  based on  $G$ ? How large were the latent higher-order interactions? All of the queries can be answered by computing appropriate averages over  $P(H|G)$ . As is made evident by Eq. (1), however, we first have to introduce two probability distributions so that we may compute  $P(H|G)$  at all. We now define these distributions in detail.

### A. Generative model

#### 1. Projection component

The first distribution,  $P(G|H)$ , we call the “projection component” of the model. It tells us how likely a particular network  $G$  is when the latent hypergraph  $H$  is known.

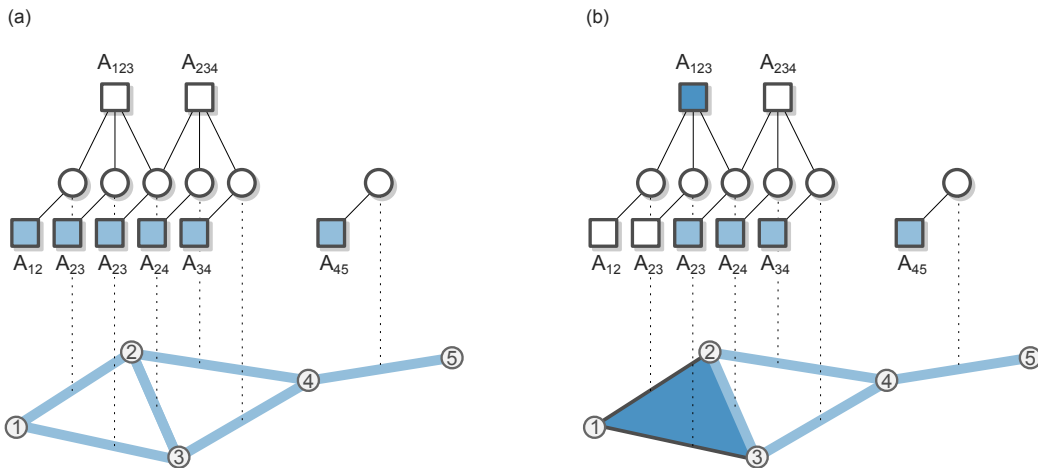


FIG. 2. Encoding of hypergraphs as factor graphs. A node (circle) is first associated with every edge of the network  $G$  shown below; this correspondence is illustrated with a dashed line in the figure. The nodes are then connected to factors (squares), one for each of the  $k$ -clique in which an edge is found. A hypergraph  $H$  can be represented by assigning counts  $A_{i_1, \dots, i_k}$  to every  $k$ -clique (factor), to encode the number of hyperedges projected on these cliques. The factor graph in (a) encodes a pure network representation of  $G$ , whereas (b) encodes a hypergraph with one higher-order interaction.

We use a direct projection component and deem two nodes connected in  $G$  if and only if these nodes jointly appear in *any* of the hyperedges of  $H$ .

This modeling choice is broadly applicable. For instance, when researchers measure the functional connectivity of two brain regions, they record a connection irrespective of whether the regions peaked as a pair or as jointly with many other regions. Likewise, surveyed social networks contain records of friendships that can be attributed to interactions between pairs of individuals, and to interactions that arise from larger groups.

Certain authors use more nuanced projection components [1, 30] and do not assume that the joint participation of two nodes in a hyperedge *necessarily* leads to measured pairwise interactions. As we have argued in the introduction, we believe that such components blur the lines between community detection and higher-order interaction reconstruction. Hence, we treat measurement as a separate issue to be handled with the methods of Refs. [32, 33], for instance.

We formalize the projection component as follows. We set  $P(G|H) = 1$  only when (i) each pair of nodes connected by an edge in  $G$  appears jointly in at least one hyperedge of  $H$ , and (ii) no two disconnected nodes of  $G$  appear in a hyperedge of  $H$ . If either of these conditions is violated, then we set  $P(G|H) = 0$ . We can express this definition mathematically as

$$P(G|H) = \begin{cases} 1 & \text{if } G = \mathcal{G}(H), \\ 0 & \text{otherwise.} \end{cases} \quad (2)$$

where we use  $G = \mathcal{G}(H)$  to say that  $H$  *projects* to  $G$ , or equivalently that (i) and (ii) hold.

Testing  $G \stackrel{?}{=} \mathcal{G}(H)$  might appear unwieldy at first, but, thankfully, there is a *factor graph* encoding of  $H$

that can help us compute the projection component efficiently [34].

To construct this factor graph, we start with a set containing one node for every edge of  $G$ . We then create a set of *factors*—a set of nodes of a second type—that contains one factor for every clique of  $G$ , including cliques included in larger ones. We finally connect these factors to the edges that they contain. For the simple network shown in Fig. 2, for example, the edge between node 1 and 2 is part of the triangle  $\{1, 2, 3\}$ , and it is therefore connected to the factor  $A_{123}$ . The edge is also part of the 2-clique  $\{1, 2\}$ , so we connect it to the factor  $A_{12}$ , too.

We use the factor graphs to encode particular hypergraphs  $H$  by assigning integers to the factors, corresponding to the number of times every hyperedge appears in  $H$ . For example,  $A_{123} = 1$  with  $A_{23} = A_{24} = A_{34} = A_{45} = 1$  would encode a hypergraph with five hyperedges, one of size 3 and four of size 2; see Fig. 2b.

It is straightforward to check whether  $G = \mathcal{G}(H)$  holds with this encoding. The first condition—all the connected nodes of  $G$  are connected by at least one hyperedge in  $H$ —can be verified by checking that every node of the factor graph is connected to at least one “active factor,” for which  $A_{i_1, \dots, i_k} > 0$ . The second condition—no pairs of disconnected nodes in  $G$  are connected by a hyperedge of  $H$ —is always satisfied, because no factor connects two disconnected nodes of  $G$ , by construction.

We note that the factor graph can be stored relatively efficiently, by first enumerating the maximal cliques—cliques not included in larger cliques—and then constructing an associative array indexed by cliques. Even though enumerating maximal clique is technically an NP-hard problem [35], state-of-the-art enumeration algorithms tend to work well on sparse empirical network data [20, 21, 36], and indeed we have found that enumer-

ation is not problematic in our experiments.

## 2. Hypergraph prior

The second part of Eq. (1),  $P(H)$ , is the ‘‘hypergraph prior.’’ Empirical hypergraphs generally have a few properties that a reasonable prior should account for [37]: the size of interactions vary; some of these interactions are repeated, and not all nodes are connected by a hyperedge. It turns out that an existing model [38], known as the Poisson Random Hypergraphs Model (PRHM), reproduces all of these properties. Hence, we adopt it as our hypergraph prior. The PRHM was initially developed to study critical phenomena in hypergraphs [38]; here, we use it to make posterior inferences about networks.

In a nutshell, the PRHM stipulates that the number of hyperedges connecting a set of nodes is a random variable, whose mean  $\lambda_k$  only depends on the size  $k$  of the set. The variable follows a Poisson distribution, such that the number of hyperedges connecting the nodes  $i_1, \dots, i_k$  equals to  $A_{i_1, \dots, i_k}$  with probability

$$P(A_{i_1, \dots, i_k} | \lambda_k) = \frac{\lambda_k^{A_{i_1, \dots, i_k}}}{A_{i_1, \dots, i_k}!} e^{-\lambda_k}, \quad (3)$$

where  $A_{i_1, \dots, i_k}$  is invariant with respect to permutation of the indexes. The PRHM also models all the hyperedges as independent. Hence, the probability of a particular hypergraph can be calculated as

$$\begin{aligned} P(H | \boldsymbol{\lambda}) &= \prod_{k=2}^L \prod_{i_1, \dots, i_k \in C_k^N} P(A_{i_1, \dots, i_k} | \lambda_k) \\ &= \prod_{k=2}^L \prod_{i_1, \dots, i_k \in C_k^N} \frac{\lambda_k^{A_{i_1, \dots, i_k}}}{A_{i_1, \dots, i_k}!} e^{-\lambda_k}, \end{aligned} \quad (4)$$

where  $L$  is the maximal hyperedge size,  $C_k^N$  denotes all possible subsets of size  $k$  of  $\{1, \dots, N\}$ , and where  $\boldsymbol{\lambda}$  refers to all the rates collectively.

Equation (4) expresses the probability of  $H$  in terms of individual hyperedges. To obtain a simpler form, we notice that the number  $E_k$  of hyperedges of size  $k$ , can be calculated as

$$E_k = \sum_{i_1, \dots, i_k \in C_k^N} A_{i_1, \dots, i_k} \quad (5)$$

and that there are precisely  $\binom{N}{k}$  terms in the product over all sets of nodes of size  $k$ . We can use these simple observations to rewrite Eq.(4) as

$$P(H | \boldsymbol{\lambda}) = \prod_{k=2}^L \frac{\lambda_k^{E_k} e^{-\binom{N}{k} \lambda_k}}{Z_k}, \quad (6)$$

where we have defined

$$Z_k = \prod_{i_1, \dots, i_k \in C_k^N} A_{i_1, \dots, i_k}! = \prod_{m=1}^{\infty} (m!)^{\eta_m^{(k)}}, \quad (7)$$

and where  $\eta_m^{(k)}$  is the number of hyperedges of size  $k$  that are repeated precisely  $m$  times.

In this form, it is clear that the parameters  $\boldsymbol{\lambda}$  control the density of  $H$  at all scales. Hence, they more or less determine the kind of hypergraphs we expect to see a priori, and therefore have a major effect on the model output. How can we choose these important parameters carefully?

We propose to a hierarchical empirical Bayes approach, in which we treat  $\boldsymbol{\lambda}$  as unknowns themselves drawn from prior distributions. We use a maximum entropy, or least informative, prior for  $\boldsymbol{\lambda}$ , because we have no information whatsoever about  $\boldsymbol{\lambda}$  a priori. The only thing we know is that these parameters take values in  $[0, \infty)$  and are modeled with a finite mean [38]. Hence, the maximal entropy prior of interest is the exponential distribution

$$P(\lambda_k | \nu_k) = \frac{e^{-\lambda_k / \nu_k}}{\nu_k}, \quad (8)$$

of mean  $\nu_k$ . We obtain a complete hyperprior for  $\boldsymbol{\lambda}$  by using independent priors for all sizes  $k$ ,  $P(\boldsymbol{\lambda} | \boldsymbol{\nu}) = \prod_{k=2}^L P(\lambda_k | \nu_k)$ . Integrating over the support of  $\boldsymbol{\lambda}$ , we find that the prior for  $H$  is now

$$\begin{aligned} P(H | \boldsymbol{\nu}) &= \int P(H | \boldsymbol{\lambda}) P(\boldsymbol{\lambda} | \boldsymbol{\nu}) d\boldsymbol{\lambda}, \\ &= \prod_{k=2}^L \frac{E_k!}{Z_k \nu_k} \left[ \frac{1}{\nu_k} + \binom{N}{k} \right]^{-(E_k+1)}, \end{aligned} \quad (9)$$

with  $\boldsymbol{\nu}$  fixed.

It might appear that we have only pushed our problem further ahead—we got rid of  $\boldsymbol{\lambda}$  but we now have a whole new set of parameters on our hands. Notice, however, that the new parameters  $\boldsymbol{\nu}$  do not have as direct an effect on  $H$ . A whole range of densities is now compatible with any choice of  $\boldsymbol{\nu}$ . And as a result, the model can assign significant probabilities to hypergraphs that project to networks of the correct density, even when the hyperprior is somewhat in error. Hence, we safely fix the new parameters  $\boldsymbol{\nu}$  with empirical Bayes without risking strongly biased results.

With these precautions in place, we use the observed number of edges  $E$  in the network  $G$  to choose  $\boldsymbol{\nu}$ . Our strategy is to equate  $E$  to the expected number of edges  $\langle E(\boldsymbol{\nu}) \rangle$  in the network  $\mathcal{G}(H)$  obtained by projecting  $H$  drawn from  $P(H | \boldsymbol{\nu})$ . This expected density can be calculated as

$$\langle E(\boldsymbol{\nu}) \rangle = \binom{N}{2} \left[ 1 - \prod_{k=2}^L (e^{-\nu_k})^{\binom{N}{k-1}} \right], \quad (10)$$

by first computing the reciprocal of the probability that two nodes are not connected by *any* hyperedge in the

hypergraph and then multiplying the result by the total number of node pairs. To set the individual values of  $\nu_k$ , we further require that all sizes contribute equally to the final density, with  $\nu_k \binom{N}{k} = \mu$  for a constant  $\mu$ . Substituting these equalities in Eq. (10), we obtain

$$\mu = (L - 1) \log \left( \frac{1}{1 - E/\binom{N}{2}} \right), \quad (11)$$

and the prior of Eq. (9) becomes

$$P(H) = \prod_{k=2}^L \frac{E_k!}{Z_k \binom{N}{k}^{E_k} \mu} \left[ \frac{N - k + 1}{k} + \frac{1}{\mu} \right]^{-(E_k+1)}. \quad (12)$$

We note that  $\mu$  diverges as the density  $E/\binom{N}{2}$  of  $G$  approaches one, correctly reflecting the fact that even an infinitely dense hypergraph could have generated the data. This divergence is a sign that our empirical prior is not well-defined in the extremely dense limit. But as we have discussed in the introduction, the empirical networks we typically encounter are sparse by construction—we need not worry about this limit in practice.

### B. Properties of $P(H|G)$

The model defined in Eqs. (2) through (12) has two important properties.

The first noteworthy property is that the model assigns a higher posterior probability to hypergraphs without repeated hyperedges, even though the prior  $P(H)$  allows for duplicates. An explicit calculation of how  $P(H|G)$  scales with the number of duplicated hyperedges can illustrate this fact. Indeed, consider a hypergraph  $H_0$  with no repeated hyperedges, for which  $P(G|H_0) = 1$ . Write as  $\alpha$  the fraction of  $k$ -cliques connected by a hyperedge in  $H_0$ , and consider an experiment in which an average of  $\beta \geq 0$  additional hyperedges are placed “on top of” the hyperedges of size  $k$  already present in  $H_0$ . In these hypergraphs, the expected number of hyperedges of size  $k$  is  $E_k = \alpha(1 + \beta) \binom{N}{k}$  and  $\log Z_k$  is approximated by

$$\sum_{i_1, \dots, i} \log A_{i_1, \dots, i} \approx \alpha \binom{N}{k} \log(1 + \beta),$$

see Eq. (7). Substituting our various formula in the logarithm of  $P(H)$ , and using the Stirling approximation  $\log n! \approx n \log n - n$ , we find that

$$\log P(H|G) \sim \alpha(1 + \beta) \binom{N}{k} \log \left( \frac{\alpha}{\frac{N+k-1}{k} + \frac{1}{\mu}} \right).$$

From this equation we can determine that the log-posterior  $\log P(H|G)$  decreases with growing  $\beta$ , because  $\alpha \in [0, 1]$ , and  $1 < k \leq L \leq N$  with  $\mu > 0$  by definition. Furthermore we have  $P(G|H) = 1$  by construction, which implies that the scaling of the prior determines the

scaling of the posterior. Hence, the hypergraphs  $H$  generated by adding duplicated hyperedges to  $H_0$ —that is by increasing  $\beta$ —are less likely than  $H_0$ .

A second noteworthy property of the model is that it favors *sparser* hypergraphs: as long as  $P(G|H) = 1$ , the fewer hyperedges, the better. To make this observation precise, suppose we have a hypergraph  $H_m$  that can be termed “minimal” for  $G$ : every edge of  $G$  is covered by exactly one hyperedge of  $H_m$  and no more. We observe that we cannot improve on the posterior probability of  $H_m$  by adding a hyperedge, even when this new hyperedge does not fully repeat an existing one. Indeed, consider the hypergraph  $H'_m$  created by adding a hyperedge of size  $k$  to  $H_m$ . (For example, we could add a hyperedge of size 3 on a triangle whose sides were already covered by edges, but did not yet participate in any larger hyperedge together.) By direct calculation, the ratio of posterior probability for  $H'_m$  and  $H_m$  equals

$$\frac{P(H'_m|G)}{P(H_m|G)} = \frac{E_k + 1}{\binom{N}{k} \left( \frac{N+k-1}{k} + \frac{1}{\mu} \right)}.$$

This ratio is smaller than one: the minimal property of  $H_m$  implies that  $E_k < \binom{N}{k}$ , and the term in the parenthesis is greater than one because  $N \gg k$ . As a result, adding a spurious hyperedge to a minimal hypergraph decreases the posterior probability.

As a corollary of the two above observations, we conclude that the “minimal hypergraphs” are high-quality local maxima of  $P(H|G)$ . We cannot simply pick one of these optima as our reconstruction, however, because there may exist multiple ones of comparable quality. Further, non-optimal hypergraphs may account for a significant fraction of the posterior probability in principle. Instead, we handle these possibly conflicting descriptions by combining them.

### C. Posterior estimation

In our Bayesian framework, posterior estimation boils down to computing arbitrary expectations of the posterior distribution  $P(H|G)$ . For example, the expected number of hyperedges of size  $k$  can be computed as  $\langle E_k \rangle = \sum_H E_k(H) P(H|G)$ . More generally, we are interested in averages of the form

$$\langle f(H) \rangle = \sum_H f(H) P(H|G) \quad (13)$$

for arbitrary functions  $f$  that map hypergraphs to vectors or scalars.

The summation in Eq. (13) is unfortunately intractable: the set of possible hypergraphs grows exponentially in size with both the number of nodes and the maximal size of the hyperedges. Hence, we propose a Markov Chain Monte-Carlo (MCMC) algorithm to evaluate Eq. (13). This kind of approach generates a random walk over the space of all hypergraphs, with limiting distribution that is identical to  $P(H|G)$ . We use the

Metropolis-Hastings (MH) construction to implement the random walk. It consists of proposing a move from  $H$  to  $H'$  with probability  $Q(H \leftarrow H')$ , and accepting it with probability [39]

$$\begin{aligned} a &= \min \left\{ 1, \frac{Q(H \leftarrow H') P(H'|G)}{Q(H' \leftarrow H) P(H|G)} \right\}, \\ &= \min \left\{ 1, \frac{Q(H \leftarrow H') P(G|H')P(H')}{Q(H' \leftarrow H) P(G|H)P(H)} \right\}. \end{aligned} \quad (14)$$

We use the factor graph representation (see Fig. 2) to define the Monte Carlo moves. All our moves alter one of the factors  $A_{i_1, \dots, i_k}$ , encoding the number of hyperedges that connect nodes  $i_1, \dots, i_k$  (see Sec. II A 1). We rely on the factor nodes associated with maximal cliques—hereafter “maximal factor nodes”—to guide the moves.

For every move, we begin by choosing a maximal factor node uniformly at random from the set of all such nodes. We select a size  $\ell$  uniformly at random from  $\{2, 3, \dots, k\}$  where  $k$  is the size of the clique corresponding to the current maximal factor. Then we select one of the subfactors  $A_{i_1, \dots, i_\ell}$  of size  $\ell$  uniformly at random, among the  $\binom{k}{\ell}$  factors of that size, and we update the selected factors as either  $A'_{i_1, \dots, i_\ell} = A_{i_1, \dots, i_\ell} + 1$  or  $A'_{i_1, \dots, i_\ell} = A_{i_1, \dots, i_\ell} - 1$  (with probability 1/2). If  $A_{i_1, \dots, i_\ell}$  was already equal to zero, we force  $A'_{i_1, \dots, i_\ell} = A_{i_1, \dots, i_\ell} + 1$ . Therefore we have that

$$\frac{Q(H \leftarrow H')}{Q(H' \leftarrow H)} = \begin{cases} 1 & \text{if } A_{i_1, \dots, i_\ell} > 0, \\ 1/2 & \text{if } A_{i_1, \dots, i_\ell} = 0, \\ 2 & \text{if } A'_{i_1, \dots, i_\ell} = 0. \end{cases} \quad (15)$$

Finally, we check whether  $P(G|H) = 1$  using the factor representation, and compute the ratio  $P(H')/P(H)$  to obtain the acceptance probability  $a$ . We test for acceptance and, if the move is accepted, we record the update. Otherwise, we do nothing.

Building on our observations about the properties of  $P(H|G)$ , we select as our initialization the hypergraph with one hyperedge for every maximal clique of  $G$ . This starting point is not a known optimum of  $P(H|G)$ , but it is close to all of them (see Sec. II B). Hence, this initialization allows for fast convergence to the equilibrium and the exploration of many optima when they are accessible.

A reference C++ implementation of the algorithm is freely available as part of the `graph-tool` Python library [40].

### III. RESULTS

#### A. Planted higher-order interaction recovery

To develop an intuition for the workings of our method, we first use the algorithm to uncover higher-order interactions in synthetic data generated in a controlled environment. We create a hypergraph that comprises large hyperedges, and add several random edges to the hypergraph to create a “noisy” hypergraph  $\tilde{H}$ . We then

project it to obtain a network  $\mathcal{G}(\tilde{H})$ , which we feed to our recovery algorithm as input. Our goal in this experiment is to find the hypergraph  $H^*$  that maximizes the posterior probability  $P(H|\mathcal{G}(\tilde{H}))$  (we do not use the full samples given by our MCMC algorithm just yet). We can consider the experiment successful if  $H^*$  contains all the higher-order interactions planted in  $\tilde{H}$ .

The results of this experiment are reported in Fig. 3. At the bottom of Fig. 3a, we show a typical example of what the projected networks  $\mathcal{G}(\tilde{H})$  looks like when there are very few added random edges. In this regime, the recovered higher-order interactions (in blue) correspond perfectly to those planted in  $\tilde{H}$ . For the sake of comparison, we also generate an equivalent random network, obtained by completely rewiring the edges of  $\mathcal{G}(\tilde{H})$ , see the top of Fig. 3a. This network has the same number of edges as  $\mathcal{G}(\tilde{H})$  but is otherwise unstructured [41]. As expected, we find no higher-order interactions beyond the random triangles that occur at this density [42].

If we add many more random edges, we obtain the results shown in Fig. 3c. Again, we can recover the planted higher-order interactions, but we also start to find additional ones, due to the appearance of “random triangles” formed by triplets of edges added at random [43]. Is it a failure of the method? How might we understand these results?

The *minimum description length* (MDL) interpretation of Bayesian inference offers a simple explanation for our results [44, 45]. In a nutshell, the MDL is the number of bits that a receiver and a sender with shared knowledge of the model  $P(G, H)$  would need to communicate the network  $G$  to one another. This communication costs can be minimized by finding a hypergraph  $H^*$  that is both cheap to communicate and projects to  $G$ ; receivers who know  $P(G, H)$  also know that they can project  $H^*$  to find  $G = \mathcal{G}(H^*)$ . From this communication perspective, hypergraphs with as few hyperedges as possible are good candidates because they are cheaper to send [26]. The connection with Bayesian inference is that  $H^*$  happens to coincide with the hypergraph which maximizes the posterior probability  $P(H|G)$  (see Appendix A for a detailed discussion). Hence, maximum a posteriori inference is equivalent to compression.

With the MDL interpretation in mind, the results of our experiment become clear. In Fig. 3b, we plot the description length provided by our model, for levels of randomness that interpolate between the easy regime shown in Fig. 3a, and the much more random regime appearing in Fig. 3c. We find that the model compresses those networks that have planted interactions much better than their randomized equivalents. These results make intuitive sense: networks with planted interactions contain large cliques, and these cliques can be harnessed to communicate regularities in  $G$ . As can be expected, these savings disappear once the large cliques are destroyed by rewiring.

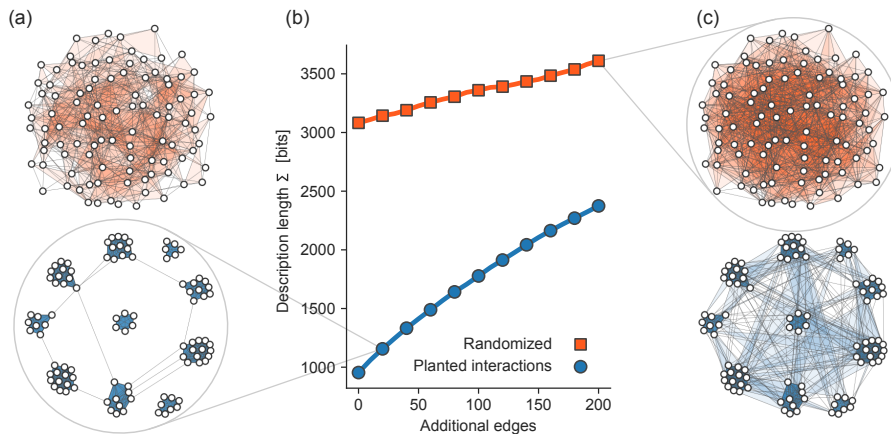


FIG. 3. Reconstruction in random networks with and without higher-order interactions. **(a)** Two networks, one obtained by projecting a hypergraph of 10 disjoint hyperedges of unequal sizes (bottom), and the other obtained by drawing uniformly from all networks with the same number of edges (top). **(b)** Minimal description length (MDL)  $\Sigma$  of the networks as a function of the number of additional, chosen uniformly at random from the set of non-edges. **(c)** The two networks with 200 additional edges. In panel (a) and (c), we use solid colors to highlight the interactions of sizes greater than 5 uncovered by maximizing  $P(H|G)$ . Smaller interactions—of size 3, 4, and 5—are highlighted with a lighter shade. The MDLs are averaged over 10 independent realizations of the network generation and inference processes.

## B. Empirical systems: a detailed case study

We consider a small empirical dataset, the football network [46], as our second example. The nodes of this network represent teams playing in Division I-A of the NCCA (now the NCAA Division I Football Bowl Subdivision), and two teams are connected if they played at least one game during the regular season of Fall 2000. The relationships between teams are viewed through the lens of pairwise interactions, but higher-order phenomena shape the system. For example, the teams of a conference all play each other during a season. Other higher-order phenomena such as geography also intervene: teams in different conferences are likely to meet during the regular season if they are in close-by states. There might also be more subtle phenomena like historical rivalries that survived conference changes.

In Fig. 4 we show the interactions that our method uncovers when we look for the single best higher-order description  $H^*$ . We find a large number of interactions that are not pairwise: 86 of the hyperedges of  $H^*$  involve more than 2 nodes.

The higher-order interactions uncovered by our method are not merely the maximal cliques of  $G$  (see Fig. 4a). We argue that *interlocked maximal cliques*—cliques that share edges—are the reason why these descriptions differ. When two maximal cliques interlock, the hypergraph constructed directly from maximal cliques contains two overlapping hyperedges. This choice is wasteful from a compression perspective: the edges in the intersection of the two cliques are part of two hyperedges, and therefore contribute twice to the description length  $\Sigma = -\log P(H)$ . Our method instead looks for a more parsimonious description of the data. In doing so, it can identify trade-offs and, for example, represent

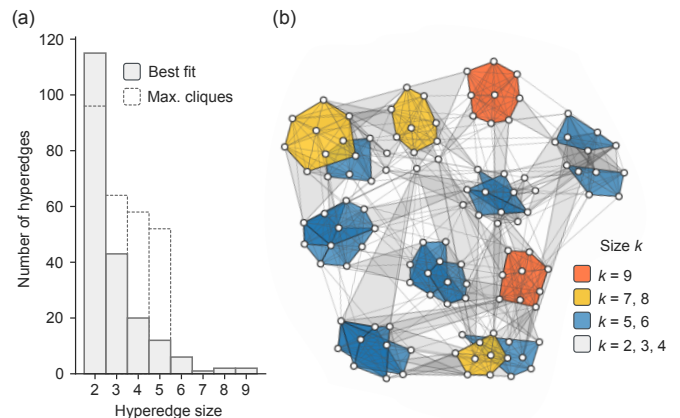


FIG. 4. Higher-order interactions uncovered in the network of American football games between teams of the Division I-A of the NCCA [46]. This undirected network has 115 nodes and 613 edges. **(a)** Size distribution of the hyperedges of the hypergraph  $H^*$  that maximizes the posterior probability  $P(H|G)$  or, alternatively, minimizes the description length (DL) of  $G$ . Also shown is the distribution of hyperedge sizes for the hypergraph constructed by assigning a hyperedge to every maximal clique of  $G$ . **(b)** Visualization of the hyperedges present in  $H^*$ , color-coded by size.  $H^*$  has no repeated hyperedges, due to the properties of  $P(H^*|G)$  analyzed in Sec. II B.

one of the two cliques as a higher-order interaction and break down the other as a series of smaller interactions, thereby avoiding redundancies. These trade-offs culminate into much better compression: we find a hypergraph  $H^*$  with a description length of 4123.3 bits, which represents a 33.6% saving over the description length of the maximal cliques hypergraph (6208.5 bits).

As we have discussed in Sec. II C, our method pro-

vides complete estimation procedures, beyond maximum a posteriori estimation. For example, a quantity that is of particular interest is the posterior probability that a set of nodes is connected by at least one hyperedge [32], once we account for the full distribution over hypergraphs  $P(H|G)$ . By computing this probability for all sets of nodes with a non-negligible connection probability, we can encode the probabilistic structure of  $H$  in a compact way [47], with a few probabilities only.

In practice, we evaluate the connection probabilities by generating samples from  $P(H|G)$  and counting the samples in which a set of interest is connected by at least one hyperedge (recall that the model defines a distribution over hypergraph with repeated hyperedges). Mathematically this is computed as

$$P(X_{i_1, \dots, i_k} = 1|G) = \frac{1}{n} \sum_{\ell=1}^n X_{i_1, \dots, i_k}(H_\ell), \quad (16)$$

where  $H_1, \dots, H_n$  are  $n$  hypergraphs sampled from  $P(H|G)$ , and where  $X_{i_1, \dots, i_k}(H) = \mathbb{1}_{A_{i_1, \dots, i_k} \geq 1}$  is a presence/absence variable, equal to 1 if and only if there is at least one hyperedge connecting nodes  $i_1, \dots, i_k$  in hypergraph  $H$ .

Applying this technique to the Football data, we find that many of the hyperedges of  $H^*$  have a presence probability close to 1, even once we account for the full distribution over hypergraphs. The hypergraph is not reconstructed with absolute certainty, however. Observing that probabilities  $P(X_{i_1, \dots, i_k} = 1|G)$  close to 1 or 0 both indicate confidence in the presence/absence of edge, we define a certainty threshold  $\alpha$  and classify all hyperedges with existence probabilities in  $[\alpha/2, 1 - \alpha/2]$  as uncertain. With a threshold of  $\alpha = 0.05$ , we find 6 uncertain triangles (hyperedges on 3 nodes) and 5 uncertain edges in the Football data.

To go beyond a simple threshold analysis, we compute the entropy of the probabilities  $\hat{p} := P(X_{i_1, \dots, i_k} = 1|G)$ , defined as

$$S(\hat{p}) = -\hat{p} \log_2 \hat{p} - (1 - \hat{p}) \log_2 (1 - \hat{p}). \quad (17)$$

The entropy provides a useful transformation of  $\hat{p}$  because it grows as  $\hat{p}$  moves away from the extremes  $\hat{p} = 0, 1$ , with a maximum of  $S = 1$  at  $\hat{p} = 1/2$ , the point of maximal uncertainty. The distribution of entropy is shown in Fig. 5a for the Football data. The figure shows that while the majority of hyperedges are ‘‘certain’’ (i.e., their entropy is greater than  $S^* \approx 0.169$  corresponding to  $\alpha = 0.05$ ), making the certainty criterion slightly more stringent would add many more uncertain hyperedges to the ones we already have.

In Fig. 5b, we show the location of the uncertain hyperedges in  $H$ . We observe that these uncertain hyperedges are co-located. The minimality properties of  $P(H|G)$  discussed in Sec. II B can explain these results. Hypergraphs that have a sizable posterior probability are typically sparse and include as few hyperedges as possible. But they also need to ‘‘cover’’ the whole graph, meaning

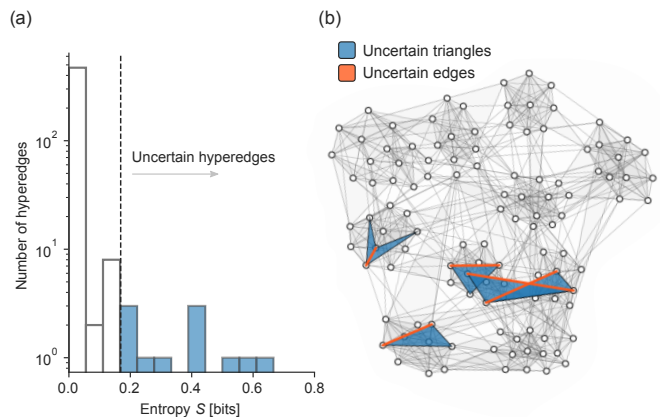


FIG. 5. Uncertain higher-order interactions uncovered in the network of American football games also analyzed in Fig. 4. (a) Distribution of the entropy of the presence/absence variables  $X_{i_1, \dots, i_k} = \mathbb{1}_{A_{i_1, \dots, i_k} \geq 1}$ . The entropy quantifies the variability of hyperedges: sets of nodes that are connected in nearly all—or almost none—of the samples have low entropy. We deem as uncertain a hyperedge that has a probability  $p \in [\alpha/2, 1 - \alpha/2]$  of being present, with  $\alpha = 0.05$ . Note that we only show the entropy for the sets of nodes that were connected at least once in our Monte Carlo samples; a large number of hyperedges, of entropy zero, are never seen in our samples. (b) Visualization of the uncertain hyperedges. Certain hyperedges are shown in light gray. All results are computed with 2,000 Monte Carlo samples from  $P(H|G)$  each separated by 2,000 complete sweep of the factor graph.

than at every edge of  $G$  needs to appear as a subset of at least one hyperedge  $H$  (due to the constraint  $G = \mathcal{G}(H)$ ). Co-located uncertain triangles and hyperedges are hence the result of competing solutions of roughly equal qualities, that cover a specific part of the hypergraph with hyperedges of different sizes.

### C. Empirical systems: systematic analysis

For our third and final example, we apply our method to 16 network data sets, taken from various representative scientific domains and structural classes [11, 14, 46, 48–59]. We list these networks in Table I of the appendix, alongside the detailed results of the experiment that follows.

For each empirical network in our list, we first search for the hypergraph  $H^*$  that maximizes  $P(H|G)$ , as we have done in our two previous examples. This search gives us a minimum description length  $\Sigma$ . For the sake of comparison, we also compute the description length  $\Sigma'$  that we would obtain if we were to use the maximum clique decomposition to construct  $H$  naively. We note that  $\Sigma'$  cannot be smaller than  $\Sigma$  because it is the description length of the starting point of the MCMC algorithm—at best, the algorithm cannot improve on  $\Sigma'$ , and we then have  $\Sigma = \Sigma'$ . The difference  $\Sigma' - \Sigma$  gives the compression factor or, in other words, the number of

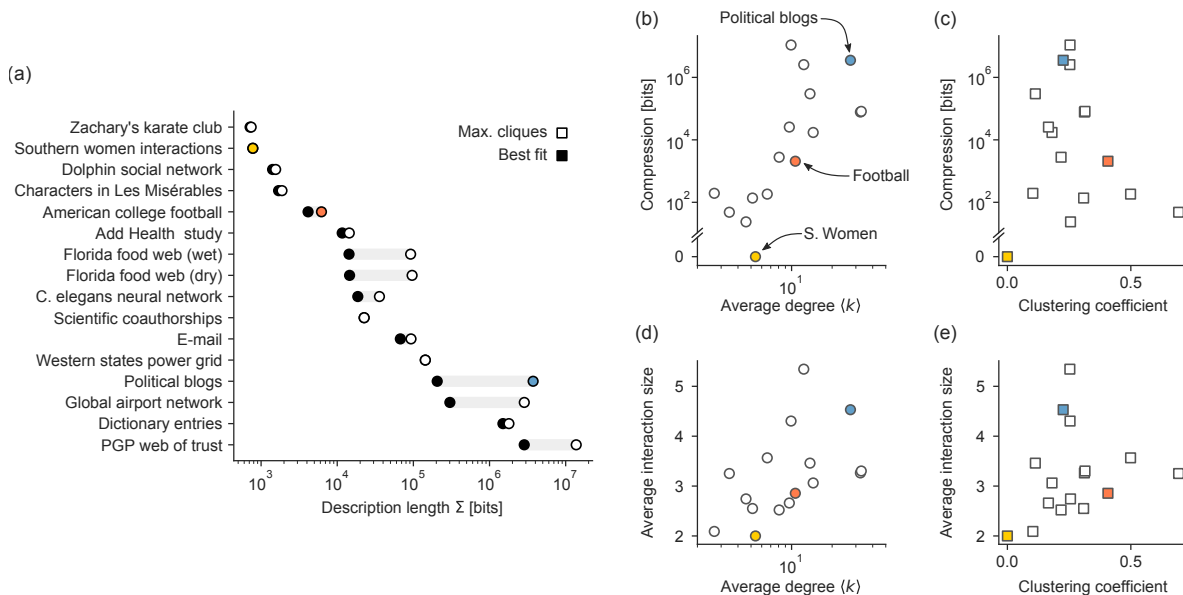


FIG. 6. Analysis of several empirical networks. A few datasets are highlighted with colors: the Southern women interaction data [48] (yellow), the Football data of Sec. III B [46] (orange), and political blogs [49] (blue). (a) Description length of the hypergraph  $H$  whose hyperedges are the maximal cliques of  $G$ , compared with the MDL found with our method. (b,c) Compression, defined as the difference in description length, as a function of the average degree and clustering coefficient [2]. (d,e) Interaction size, averaged over all interactions in  $H^*$ , as a function of the average degree and clustering coefficient. Detailed numerical results are reported in Table I of the Appendix.

bits we save by using the best hypergraph instead of a hypergraph of maximal cliques.

In Fig. 6a, we show the description lengths of the networks in our collection of datasets. We observe a broad range of outcomes. Compression of multiple orders of magnitude is possible in some cases, like with the political blogs data [49] highlighted in blue, while the best description is directly the maximal cliques in others, like with the Southern women interaction data [48] highlighted in yellow. We find that the average degree of the nodes correlates with compression (Kendall’s  $\tau = 0.53$ ); see Fig. 6b. This result is expected: the denser a network, the more likely it is that interlocking cliques are present, and therefore that a parsimonious description can be obtained by optimizing over  $P(H|D)$ . The average local clustering coefficient  $\langle C \rangle$  [2] is not correlated with compression, however ( $\tau = -0.07$ ); see Fig. 6c. Local clustering quantifies the density of closed triangles in the neighborhood of a node and is, as such, a proxy for the density of cliques. However, as our results show,  $\langle C \rangle$  fails to capture the correct type of redundancy necessary for good compression with our model.

We note that clustering nonetheless predicts the absence of compression well: If  $\langle C \rangle = 0$ , then there are no closed triangles in  $G$ , and it is impossible to compress the network with our method—there are no cliques, and therefore no higher-order interactions in the data. The Southern Women [48] falls in this category because it is a bipartite network.

In Figs. 6d and 6e, we show the size of the higher-order interactions found by our method, averaged over

the hyperedges of  $H^*$ . We again observe a wide range of outcomes. As a sanity check, we can confirm that the incompressible network has an average interaction size of 2. All hypergraphs are just networks in this case and therefore have no higher-order interactions. Other datasets yield hypergraphs with large interactions on average, involving as many as 5 nodes the airport network. The correlation between local properties and interaction size is not as strong as with compression, but there are some dependencies ( $\tau = 0.40$  and  $\tau = 0.27$  for the degree and local clustering, respectively). These might be partly explained by constrained on the possible values that the average interaction size  $\langle s \rangle$  can adopt. For instance, to have an average size  $\langle s \rangle$ , a network must have an average degree of at least  $\langle s \rangle - 1$ . Likewise, some level of clustering is required to obtain large interactions.

Summarizing these results, we find that some level of compression is always possible, except when the network has no clustering whatsoever. Furthermore, we find that a high average degree is related to more compression and larger higher-order interactions. Finally, we find that some minimal level of clustering is necessary for compression, but that results vary otherwise.

#### IV. CONCLUSION

Higher-order interactions shape most relational data sets [7, 31], even when they are not explicitly encoded. In this work, we have shown that it is possible to re-

cover these interactions from data. We have argued that while the problem is ill-defined, one can introduce regularization in the form of a Bayesian generative model, and obtain a principled recovery method.

The method we have proposed here is undoubtedly one of the simplest instantiations of the broader idea of uncovering higher-order interactions in empirical relational data. There are many ways in which one could expand on the method. On the modeling front, for example, it would be worthwhile to study the interplay of the projection component  $P(G|H)$  of Eq. (2) and inference: can it be defined in a way that does not turn higher-order interaction discovery into overlapping community detection? The hypergraph prior, too, could most likely be expanded in interesting directions. The Poisson Random Hypergraphs Model (PRHM) we have used is simple; it would be interesting to study models that include degree heterogeneity as part of the reconstruction [60–62]. One could also envision a simplicial analog to these models, leading to probabilistic simplicial complex recovery [63]. Finally, it would be interesting to explore the connection between different forms of regularizations that make the problem well-defined.

On the technical front, it will be interesting to see whether more refined MCMC methods can lead to better inference results. Our proposed move-set is, after all, among the simplest one can propose for the problem. Another interesting avenue of research will be to harness the known properties of  $P(H|G)$ , reviewed in Sec. II B, to construct efficient inference algorithms, and perhaps connect the method to algorithms in the graph theory of clique covers.

The higher-order interaction data we need to inform the development of higher-order network science [7] are often inaccessible. Our methods provide the tools needed to extract higher-order structures from much more accessible and abundant relation data. With this work, we hope to have shown that moving to principled techniques is possible, and that *ad hoc* reconstruction methods should be avoided, in favor of those based on information-theoretic parsimony and statistical evidence.

## ACKNOWLEDGMENTS

This work was funded in part by the James S. McDonnell Foundation (JGY) and the Sanpaolo Innovation Center and from Compagnia San Paolo, ADnD project (GP).

## Appendix A: Minimum description length

We use the minimum description length (MDL) principle to quantify the quality of our inference. The MDL relies on an information-theoretic interpretation of the posterior distribution  $P(H|G)$  to yield principled model

comparison methods [44, 45] and is justified as follows. We first take the logarithm of the posterior distribution and obtain

$$-\log_2 P(H|G) = -\log_2 P(H) - \log_2 P(G|H) + C \quad (\text{A1})$$

where  $C$  depends only on  $G$ —a constant for inference purposes. The right-hand of Eq. (A1) can be interpreted as the sum of two information-theoretic quantities. The first,  $L(H) = -\log_2 P(H)$ , is the number of bits needed to specify the hypergraph  $H$  when a receiver and a sender both agree that  $H$  was generated from the PRHM of Sec. II. The second quantity,  $L(G|H) = -\log_2 P(G|H)$ , is the number of bits needed to specify the network  $G$  once the receiver and sender have a shared knowledge of  $H$ . Under our model, this quantity appropriately evaluates to 0 bits when  $G = \mathcal{G}(H)$ : there is only one projection  $\mathcal{G}(H)$ , such that no information is needed to specify the operation. The receiver can apply the projection operation with no outside information and correctly find  $G$ . With these equivalences in place, we calculate the description length as

$$\Sigma = -\log_2 P(H^*), \quad (\text{A2})$$

where  $H^*$  is the hypergraph that maximizes  $P(H)$  while satisfying  $P(G|H^*) = 1$ .

Equation (A2) is the length of the shortest possible description that one can give of  $G$ , using a shared knowledge of our model. A good model is one that allows for the parsimonious description of data by exploiting its regularities. Viewed from this perspective, our model achieves savings by describing the network in terms of its cliques, which is much cheaper than enumerating all of its edges.

One of the advantages of the MDL approach is that it naturally accounts for the trade-off between model complexity and accuracy. Indeed, it does not cost a lot to communicate the parameters of a simple model, but simple models usually have a diffuse distribution over the space of possible data, such that the informational cost of specifying the data is itself large. Complex models are instead associated with a large baseline of communication costs: specifying the parameters takes a lot of information. These models, however, can then leverage the parameters to communicate the data at little additional costs. Our model makes use of this strategy and pays all of its information cost via the hypergraph prior.

Dataset	$E$	$\langle k \rangle$	$C$	MDL [bits]	Clique DL [bits]	$\langle s \rangle$
Zachary's karate club [50]	78	4.6	0.26	717	740	2.74
Southern women interactions [48]	89	5.4	0.00	778	778	2.00
Dolphin social network [51]	159	5.1	0.31	1,416	1,553	2.55
Characters in Les Misérables [52]	254	6.6	0.50	1,698	1,881	3.57
American college football [46]	613	10.7	0.41	4,139	6,208	2.86
Add Health study [14]	1,136	8.1	0.22	11,618	14,396	2.52
Florida food web (wet) [53]	2,075	32.4	0.31	14,281	91,996	3.26
Florida food web (dry) [53]	2,106	32.9	0.31	14,521	96,200	3.30
<i>C. elegans</i> neural network [11]	2,148	14.5	0.18	18,619	35,829	3.06
Scientific coauthorships [54]	2,742	3.5	0.69	22,525	22,573	3.25
E-mail [55]	5,451	9.6	0.17	67,433	93,088	2.66
Western states power grid [56]	6,594	2.7	0.10	143,233	143,427	2.09
Political blogs [49]	16,714	27.4	0.23	205,489	3,737,574	4.53
Global airport network [57]	20,232	12.3	0.25	301,459	2,860,031	5.34
Dictionary entries [58]	91,471	13.7	0.11	1,499,765	1,798,071	3.46
PGP web of trust [59]	197,150	9.9	0.25	2,855,554	13,753,620	4.30

TABLE I. Empirical networks used in this work. For each network, we report the size (number of edges)  $E$ , the average degree  $\langle k \rangle$ , the average clustering coefficient  $C$ , the minimum description length, the description length of the hypergraph constructed with maximal cliques, and the average interaction size.

- 
- [1] S. A. Williamson and M. Tec, Random clique covers for graphs with local density and global sparsity. Preprint [arXiv:1810.06738](https://arxiv.org/abs/1810.06738) (2018).
- [2] M. Newman, *Networks*. Oxford University Press, 2nd edition (2018).
- [3] O. Frank and D. Strauss, Markov graphs. *J. Am. Stat. Assoc.* **81**, 832–842 (1986).
- [4] D. Iacobucci and S. Wasserman, Social networks with two sets of actors. *Psychometrika* **55**, 707–720 (1990).
- [5] D. J. Watts, P. S. Dodds, and M. E. J. Newman, Identity and search in social networks. *Science* **296**, 1302–1305 (2002).
- [6] M. E. J. Newman, Properties of highly clustered networks. *Phys. Rev. E* **68**, 026121 (2003).
- [7] F. Battiston, G. Cencetti, I. Iacopini, V. Latora, M. Lucas, A. Patania, J.-G. Young, and G. Petri, Networks beyond pairwise interactions: structure and dynamics. *Phys. Rep.* (2020).
- [8] M. Latapy, C. Magnien, and N. Del Vecchio, Basic notions for the analysis of large two-mode networks. *Soc Netw.* **30**, 31–48 (2008).
- [9] P. Pollner, G. Palla, and T. Vicsek, Preferential attachment of communities: The same principle, but a higher level. *Europhys. Lett.* **73**, 478 (2005).
- [10] L. Hébert-Dufresne, E. Laurence, A. Allard, J.-G. Young, and L. J. Dubé, Complex networks as an emerging property of hierarchical preferential attachment. *Phys. Rev. E* **92**, 062809 (2015).
- [11] J. G. White, E. Southgate, J. N. Thomson, and S. Brenner, The structure of the nervous system of the nematode *Caenorhabditis elegans*. *Philos. Trans. R. Soc. B* **314**, 1–340 (1986).
- [12] R. Atkin, *Mathematical Structure in Human Affairs*. Heinemann (1974).
- [13] J. Grilli, G. Barabás, M. J. Michalska-Smith, and S. Allesina, Higher-order interactions stabilize dynamics in competitive network models. *Nature* **548**, 210–213 (2017).
- [14] M. D. Resnick *et al.*, Protecting adolescents from harm: findings from the national longitudinal study on adolescent health. *J. Am. Med. Assoc.* **278**, 823–832 (1997).
- [15] S. Fortunato, Community detection in graphs. *Phys. Rep.* **486**, 75–174 (2010).
- [16] J. Xie, S. Kelley, and B. K. Szymanski, Overlapping community detection in networks: The state-of-the-art and comparative study. *ACM Comput. Surv.* **45**, 1–35 (2013).
- [17] A. Patania, F. Vaccarino, and G. Petri, Topological analysis of data. *EPJ Data Sci.* **6** (2017).
- [18] G. Petri, M. Scolamiero, I. Donato, and F. Vaccarino, Networks and cycles: a persistent homology approach to complex networks. In *Proceedings of the European Conference on Complex Systems 2012*, pp. 93–99 (2013).
- [19] G. Petri, M. Scolamiero, I. Donato, and F. Vaccarino, Topological strata of weighted complex networks. *PLOS ONE* **8**, e66506 (2013).
- [20] C. Bron and J. Kerbosch, Algorithm 457: Finding all cliques of an undirected graph. *Commun. ACM* **16**, 575–577 (1973).
- [21] E. Tomita, A. Tanaka, and H. Takahashi, The worst-case time complexity for generating all maximal cliques and computational experiments. *Theor. Comput. Sci.* **363**, 28–42 (2006).
- [22] S. Jain and C. Seshadhri, A fast and provable method for estimating clique counts using Turán's theorem. In *Proceedings of the 26th International Conference on World Wide Web*, pp. 441–449 (2017).

- [23] P. Erdős, A. W. Goodman, and L. Pósa, The representation of a graph by set intersections. *Can. J. Math.* **18**, 106–112 (1966).
- [24] B. C. Coutinho, A.-K. Wu, H.-J. Zhou, and Y.-Y. Liu, Covering problems and core percolations on hypergraphs. *Phys. Rev. Lett.* **124**, 248301 (2020).
- [25] A. E. Wegner, Subgraph covers: an information-theoretic approach to motif analysis in networks. *Phys. Rev. X* **4**, 041026 (2014).
- [26] D. Koutra, U. Kang, J. Vreeken, and C. Faloutsos, Vog: Summarizing and understanding large graphs. In *Proceedings of the 2014 SIAM international conference on data mining*, pp. 91–99, SIAM (2014).
- [27] Y. Liu, T. Safavi, N. Shah, and D. Koutra, Reducing large graphs to small supergraphs: a unified approach. *Soc. Netw. Anal. Min.* **8**, 17 (2018).
- [28] G. B. Davis and K. M. Carley, Clearing the fog: Fuzzy, overlapping groups for social networks. *Soc. Netw.* **30**, 201–212 (2008).
- [29] E. M. Airolidi, D. M. Blei, S. E. Fienberg, and E. P. Xing, Mixed membership stochastic blockmodels. *J. Mach. Learn. Res.* **9**, 1981–2014 (2008).
- [30] D. Barber, Clique matrices for statistical graph decomposition and parameterising restricted positive definite matrices. Preprint [arXiv:1206.3237](https://arxiv.org/abs/1206.3237) (2012).
- [31] L. Torres, A. S. Blevins, D. S. Bassett, and T. Eliassirad, The why, how, and when of representations for complex systems. Preprint [arXiv:2006.02870](https://arxiv.org/abs/2006.02870) (2020).
- [32] J.-G. Young, G. T. Cantwell, and M. E. J. Newman, Robust bayesian inference of network structure from unreliable data. Preprint [arXiv:2008.03334](https://arxiv.org/abs/2008.03334) (2020).
- [33] T. P. Peixoto, Reconstructing networks with unknown and heterogeneous errors. *Phys. Rev. X* **8**, 041011 (2018).
- [34] C. M. Bishop, *Pattern Recognition and Machine Learning*. Springer (2006).
- [35] R. M. Karp, Reducibility among combinatorial problems. In *Complexity of computer computations*, pp. 85–103, Springer (1972).
- [36] J. Fox, T. Roughgarden, C. Seshadhri, F. Wei, and N. Wein, Finding cliques in social networks: A new distribution-free model. *SIAM J. Comput.* **49**, 448–464 (2020).
- [37] S. G. Aksoy, C. Joslyn, C. Ortiz Marrero, B. Praggastis, and E. Purvine, Hypernetwork science via high-order hypergraph walks. *EPJ Data Sci.* **9** (2020).
- [38] R. W. Darling and J. R. Norris, Structure of large random hypergraphs. *Ann. Appl. Probab.* **15**, 125–152 (2005).
- [39] C. Andrieu, N. De Freitas, A. Doucet, and M. I. Jordan, An introduction to mcmc for machine learning. *Mach. Learn.* **50**, 5–43 (2003).
- [40] T. P. Peixoto, The graph-tool python library. *figshare* (2014), URL <https://graph-tool.skewed.de>.
- [41] P. Erdős and A. Rényi, On the evolution of random graphs. *Publ. Math. Inst. Hung. Acad. Sci.* **5**, 17–60 (1960).
- [42] B. Bollobás and P. Erdős, Cliques in random graphs. *Math. Proc. Camb. Philos. Soc.* **80**, 419–427 (1976).
- [43] X. Shi, L. A. Adamic, and M. J. Strauss, Networks of strong ties. *Phys. A* **378**, 33–47 (2007).
- [44] D. J. C. MacKay, *Information theory, inference and learning algorithms*. Cambridge University Press, 1st edition (2003).
- [45] P. D. Grünwald, *The Minimum Description Length Principle*. MIT Press (2007).
- [46] M. Girvan and M. E. J. Newman, Community structure in social and biological networks. *Proc. Natl. Acad. Sci. U.S.A.* **99**, 7821–7826 (2002).
- [47] P. Parchas, F. Gullo, D. Papadias, and F. Bonchi, Uncertain graph processing through representative instances. *ACM Transactions on Database Systems* **40** (2015).
- [48] A. Davis, B. B. Gardner, and M. R. Gardner, *Deep South: A social anthropological study of caste and class*. University of South Carolina Press (2009).
- [49] L. A. Adamic and N. Glance, The political blogosphere and the 2004 US election: divided they blog. In *Proceedings of the 3rd international workshop on Link discovery*, pp. 36–43 (2005).
- [50] W. W. Zachary, An information flow model for conflict and fission in small groups. *J. Anthropol. Res.* **33**, 452–473 (1977).
- [51] D. Lusseau, K. Schneider, O. J. Boisseau, P. Haase, E. Slooten, and S. M. Dawson, The bottlenose dolphin community of Doubtful Sound features a large proportion of long-lasting associations. *Behav. Ecol. Sociobiol.* **54**, 396–405 (2003).
- [52] D. E. Knuth, *The Stanford GraphBase: A platform for combinatorial computing*. Addison-Wesley, 1st edition (1993).
- [53] R. E. Ulanowicz and D. L. DeAngelis, Network analysis of trophic dynamics in South Florida ecosystems. In *US Geological Survey Program on the South Florida Ecosystem*, p. 114 (1999).
- [54] M. E. J. Newman, Modularity and community structure in networks. *Proc. Natl. Acad. Sci. U.S.A.* **103**, 8577–8582 (2006).
- [55] R. Guimera, L. Danon, A. Diaz-Guilera, F. Giralt, and A. Arenas, Self-similar community structure in a network of human interactions. *Phys. Rev. E* **68**, 065103 (2003).
- [56] D. J. Watts and S. H. Strogatz, Collective dynamics of ‘small-world’ networks. *Nature* **393**, 440 (1998).
- [57] T. P. Peixoto, Hierarchical block structures and high-resolution model selection in large networks. *Phys. Rev. X* **4**, 011047 (2014).
- [58] V. Batagelj, A. Mrvar, and M. Zaversnik, *Network analysis of texts* (2002).
- [59] O. Richters and T. P. Peixoto, Trust transitivity in social networks. *PLOS ONE* **6** (2011).
- [60] T. P. Peixoto, Latent poisson models for networks with heterogeneous density. *Phys. Rev. E* **102**, 012309 (2020).
- [61] D. Stasi, K. Sadeghi, A. Rinaldo, S. Petrović, and S. E. Fienberg,  $\beta$  models for random hypergraphs with a given degree sequence. Preprint [arXiv:1407.1004](https://arxiv.org/abs/1407.1004) (2014).
- [62] P. S. Chodrow, Configuration models of random hypergraphs. *J. Complex Netw.* **8** (2020).
- [63] J.-G. Young, G. Petri, F. Vaccarino, and A. Patania, Construction of and efficient sampling from the simplicial configuration model. *Phys. Rev. E* **96**, 032312 (2017).